Electronic Supplementary Material (ESI) for Dalton Transactions.

Supporting Information

A new polar alkaline earth−rare earth−iodate, $Ba_2Ce(IO_3)_8(H_2O)$

Xue-Ying Zhang,[a,b] Xiao-Han Zhang,[a] Bing-Ping Yang,*[,a,b] and Jiang-Gao Mao*[,a,b]

a. State Key Laboratory of Structural Chemistry, Fujian Institute of Research on the Structure of Matter, Chinese Academy of Sciences, Fuzhou 350002, China
b. University of Chinese Academy of Sciences, Beijing, 100049, China

E-mail: ybp@fjirsm.ac.cn; mjg@fjirsm.ac.cn

Supporting Information

Table S1. Crystal data and structure refinement of $Ba_2Ce(IO_3)_8(H_2O)$.

Table S2. Fractional atomic coordinates ($\times 10^4$), equivalent isotropic displacement parameters ($Å^2 \times 10^3$) and calculated bond valence sums (BVS) for $Ba_2Ce(IO_3)_8(H_2O)$. Ueq is defined as one-third of the trace of the orthogonalised Uij tensor.

Table S3. Bond lengths of $Ba_2Ce(IO_3)_8(H_2O)$.

Table S4. Calculation of the dipole moments of the IO_3 and CeO_9 polyhedrons and the net dipole moment of a unit cell of $Ba_2Ce(IO_3)_8(H_2O)$.

Table S5. Classification of existing cerium iodates.

Figure S1. Experimental and simulated powder X-ray diffraction (PXRD) patterns of $Ba_2Ce(IO_3)_8(H_2O)$.

Figure S2. Energy dispersive spectroscopy analyses for $Ba_2Ce(IO_3)_8(H_2O)$.

Figure S3. Coordination environment of $Ba(1)^{2+}$ (a) and $Ba(2)^{2+}$ (b).

Figure S4. Infrared spectrum of $Ba_2Ce(IO_3)_8(H_2O)$.

Figure S5. Calculated band structures of $Ba_2Ce(IO_3)_8(H_2O)$.

Figure S6. Photograph of $Ba_2Ce(IO_3)_8(H_2O)$ crystals.

Figure S7. Comparison of the dipole moment density and the SHG effect of the reported cerium iodate NLO materials.

Figure S8. Plot of particle size versus SHG intensity of $Ba_2Ce(IO_3)_8(H_2O)$ under laser irradiation at λ = 1064 nm.

Table S1. Crystal data and structure refinement of $Ba_2Ce(IO_3)_8(H_2O)$.

Formula	$Ba_2Ce(IO_3)_8(H_2O)$
Formula weight	1832.02
Temperature/K	150.00(10)
Crystal system	orthorhombic
Space group	$Pna2_1$
a/Å	15.5042(5)
b/Å	7.8841(3)
c/Å	19.5359(8)
α/°	90
β/°	90
γ/°	90
Volume/Å^3	2388.00(15)
Z	4
ρ_{calc}g/cm^3	5.096
μ/mm^{-1}	15.587
F(000)	3184.0
Radiation	Mo Kα (λ = 0.71073)
Independent reflections	4016 [R_{int} = 0.0407, R_{sigma} = 0.0359]
Goodness-of-fit on F^2	1.053
Final R indexes [I>=2σ (I)]	R_1 = 0.0246, wR_2 = 0.0528
Final R indexes [all data]	R_1 = 0.0277, wR_2 = 0.0548
Flack parameter	0.01(3)

[a] $R_1 = \Sigma||F_o|-|F_c||/\Sigma|F_o|$; and $wR_2 = \{\Sigma[w(F_o^2-F_c^2)^2]/\Sigma[w(F_o^2)^2]\}^{1/2}$

Table S2. Fractional atomic coordinates ($\times 10^4$), equivalent isotropic displacement parameters ($Å^2 \times 10^3$) and calculated bond valence sums (BVS) for $Ba_2Ce(IO_3)_8(H_2O)$. Ueq is defined as one-third of the trace of the orthogonalised Uij tensor.

Atom	x	y	z	U(eq)	BVS
Ce1	5557.4(6)	2557.6(8)	4462.5(5)	5.53(18)	3.457
Ba1	6710.6(6)	2546.3(10)	7572.3(5)	6.5(2)	2.228
Ba2	7806.0(6)	7624.7(10)	6280.8(5)	7.2(2)	2.156
I1	3830.1(6)	2467.0(10)	3057.0(5)	6.6(2)	4.840
I2	3828.2(6)	5892.3(11)	4556.6(5)	5.8(2)	5.009
I3	4911.3(6)	764.1(11)	6184.7(5)	7.2(2)	4.916
I4	6331.3(6)	924.0(10)	2828.6(5)	7.0(2)	4.899
I5	7392.2(6)	2488.6(10)	5729.1(5)	6.0(2)	4.772
I6	5506.8(6)	5988.8(11)	5984.5(5)	6.6(2)	5.055
I7	5629.1(6)	6077.6(11)	2934.4(5)	7.1(2)	4.907
I8	7325.5(6)	5942.6(11)	4301.6(5)	6.4(2)	4.998
O1	3762(7)	1144(14)	2299(6)	17(3)	1.794
O2	4261(6)	4365(12)	2654(6)	12(2)	2.070
O3	4833(6)	1608(12)	3431(6)	8(2)	2.047
O4	5426(8)	-611(12)	4484(7)	21(3)	1.726
O5	4186(6)	3793(12)	4250(5)	8(2)	1.920
O6	3147(7)	5158(12)	5240(5)	12(2)	2.251
O7	3035(7)	6258(13)	3902(5)	10(2)	2.201
O8	4600(6)	1711(14)	5367(5)	12(3)	1.969
O9	3837(6)	375(12)	6516(6)	13(3)	1.866
O10	5189(7)	2610(11)	6699(6)	11(2)	1.824
O11	7445(6)	648(12)	2554(6)	9(2)	2.063
O12	6543(6)	1502(13)	3723(5)	12(2)	2.106
O13	6196(7)	2982(12)	2434(5)	12(2)	1.975
O14	7488(7)	1113(12)	6466(5)	7(2)	2.235
O15	6929(6)	4303(11)	6187(5)	6(2)	1.742
O16	6383(6)	1538(12)	5398(5)	8(2)	1.899
O17	4534(7)	7236(12)	5945(6)	10(2)	1.998
O18	5336(7)	4894(12)	5176(5)	9(2)	2.080
O19	6247(7)	7570(12)	5660(6)	13(3)	2.011
O20	5807(7)	4895(13)	3727(6)	12(2)	2.003
O21	6581(7)	7407(12)	2998(6)	12(2)	1.930
O22	4856(7)	7570(12)	3294(6)	11(3)	1.877
O23	6949(6)	3931(11)	4654(5)	8(2)	1.944
O24	8144(7)	6287(12)	4954(6)	12(2)	1.853
O25	7971(6)	5169(12)	3603(5)	10(2)	1.988

Table S3. Bond lengths of $Ba_2Ce(IO_3)_8(H_2O)$.

Bond	Length/Å	Bond	Length/Å
Ce1-O3	2.426(10)	Ba2-O19	2.704(11)
Ce1-O4	2.507(10)	Ba2-O24	2.846(11)
Ce1-O5	2.375(10)	I1-O1	1.815(10)
Ce1-O8	2.402(10)	I1-O2	1.818(9)
Ce1-O12	2.262(10)	I1-O3	1.846(10)
Ce1-O16	2.371(11)	I2-O5	1.845(9)
Ce1-O18	2.335(10)	I2-O6	1.798(10)
Ce1-O20	2.369(11)	I2-O7	1.797(10)
Ce1-O23	2.443(10)	I3-O8	1.829(10)
Ba1-O1[2]	3.048(11)	I3-O9	1.814(10)
Ba1-O2[1]	2.867(10)	I3-O10	1.820(10)
Ba1-O7[1]	2.791(11)	I4-O11	1.822(10)
Ba1-O10	2.912(11)	I4-O12	1.836(10)
Ba1-O11[3]	2.774(10)	I4-O13	1.809(10)
Ba1-O14	2.720(10)	I5-O14	1.809(10)
Ba1-O15	3.059(10)	I5-O15	1.834(9)
Ba1-O21[4]	2.779(11)	I5-O16	1.852(10)
Ba1-O22[1]	2.809(11)	I5-O23	2.485(10)
Ba1-O25[4]	2.794(10)	I6-O17	1.803(10)
Ba2-O1[1]	3.287(11)	I6-O18	1.820(10)
Ba2-O6[5]	2.733(10)	I6-O19	1.810(10)
Ba2-O9[6]	2.891(10)	I7-O20	1.829(11)
Ba2-O11[3]	2.960(11)	I7-O21	1.814(10)
Ba2-O13[3]	2.747(10)	I7-O22	1.821(10)
Ba2-O14[7]	2.817(9)	I8-O23	1.825(9)
Ba2-O15	2.957(9)	I8-O24	1.819(11)
Ba2-O17[5]	2.760(10)	I8-O25	1.799(10)

Symmetry transformations used to generate equivalent atoms:[1]1-X,1-Y,1/2+Z; [2]1-X, -Y,1/2+Z; [3]3/2-X,1/2+Y,1/2+Z; [4]3/2-X, -1/2+Y,1/2+Z; [5]1/2+X,3/2-Y, +Z; [6]1/2+X,1/2-Y, +Z; [7]+X,1+Y, +Z.

Table S4. Calculation of the dipole moments of the IO_3 and CeO_9 polyhedrons and the net dipole moment of a unit cell of $Ba_2Ce(IO_3)_8(H_2O)$.

$Ba_2Ce(IO_3)_8(H_2O)$				
Polar unit (a unit cell)	Dipole moment (D)			
	x	*y*	*z*	total
$I(1)O_3$	2×(±10.91)	2×(±1.05)	4×(−8.50)	13.87
$I(2)O_3$	2×(±10.39)	2×(±10.55)	4×(−2.89)	15.09
$I(3)O_3$	2×(±9.21)	2×(±9.99)	4×(0.46)	13.59
$I(4)O_3$	2×(±10.00)	2×(±10.30)	4×(2.05)	14.50
$I(5)O_3$	2×(±11.07)	2×(±2.30)	4×(9.48)	14.75
$I(6)O_3$	2×(±3.78)	2×(±8.24)	4×(−13.36)	16.14
$I(7)O_3$	2×(±3.19)	2×(±7.42)	4×(13.26)	15.53
$I(8)O_3$	2×(±9.59)	2×(±10.71)	4×(2.99)	14.68
CeO_9	2×(±1.20)	2×(±1.42)	4×(−0.95)	2.09
Net dipole moment	0	0	10.2020	/
Net dipole moment (IO_3)	0	0	14.0202	/
Cell Volume	2388.00 Å^3			
Dipole moment density	10.2020/2388.00=0.0043 D Å^{-3}			
Dipole moment density (IO_3)	14.0202/2388.00=0.0059 D Å^{-3}			

Table S5. Classification of existing cerium iodates.

	Compound	Space group	SHG	Band gap	Ref
Ce(III)	$Ce(IO_3)_3$	$P2_1/n$	N/A	N/A	1
	$Ce(VO_3)_2(IO_3)$	$Pbcm$	N/A	1.64 eV	2
	$NaCe(IO_3)_4$	Cc	50 × α−SiO_2	2.97 eV	3
	$Ce(MoO_2)(IO_3)_4(OH)$	$P2_1$	negligible	2.41 eV	4
	$Ce_3Pb_3(IO_3)_{13}O$	$R3cH$	very weak	2.4 eV	5
	$Ce_2I_6O_{18}$	$P2_1$	9 × KDP	2.5 eV	6
Ce(IV)	$Ce(IO_3)_4{\cdot}H_2O$	$P2_1/n$	N/A	N/A	7
	$Ce(IO_3)_4$	$P4_2/n$	N/A	N/A	8
	$Ce_2(IO_3)_8(H_2O)$	$R3c$	1.3 × KDP	2.43 eV	9
	$Ce(IO_3)_2F_2{\cdot}H_2O$	$Ima2$	3 × KDP	2.6 eV	10
	$Ce_2(IO_3)_6(O)$	$Pnma$	N/A	N/A	11
	$K_8Ce_2I_{18}O_{53}$	$C2/c$	N/A	2.34 eV	12
	$Ce(IO_3)_2(SO_4)$	$P2_12_12_1$	3.5 × KDP	2.42 eV	13
	$Ce(IO_3)_2F_2$	$Pna2_1$	5.5 × KDP	2.70 eV	14
	$CaCe(IO_3)_3(IO_3F)F$	$Pna2_1$	5 × KDP	2.72 eV	15
intermediate-valent Ce(III)/Ce(IV)	$La_{0.3}Ce_9(IO_3)_{36}$	$R3c$	1.1 × KDP	2.30 eV	16
	$K_3Ce_9(IO_3)_{36}$	$R3c$	0.4 × KDP	2.30 eV	16
	$Ce_2(IO_3)_6(OH_{0.44})$	$Pnma$	N/A	N/A	11

N/A: stands for not applicable or not available

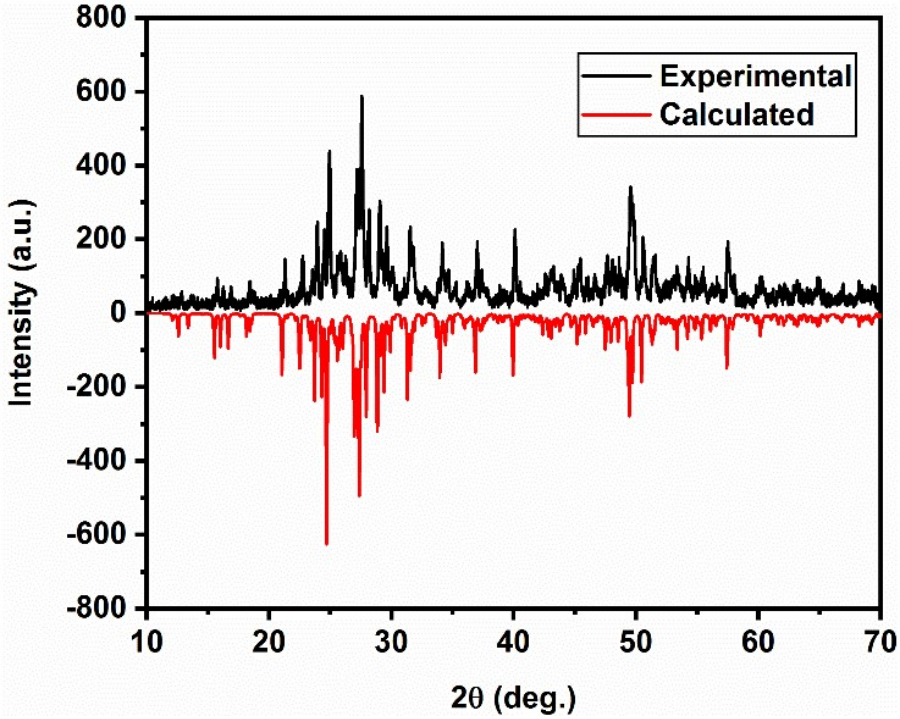

Figure S1. Experimental and simulated powder X-ray diffraction (PXRD) patterns of $Ba_2Ce(IO_3)_8(H_2O)$.

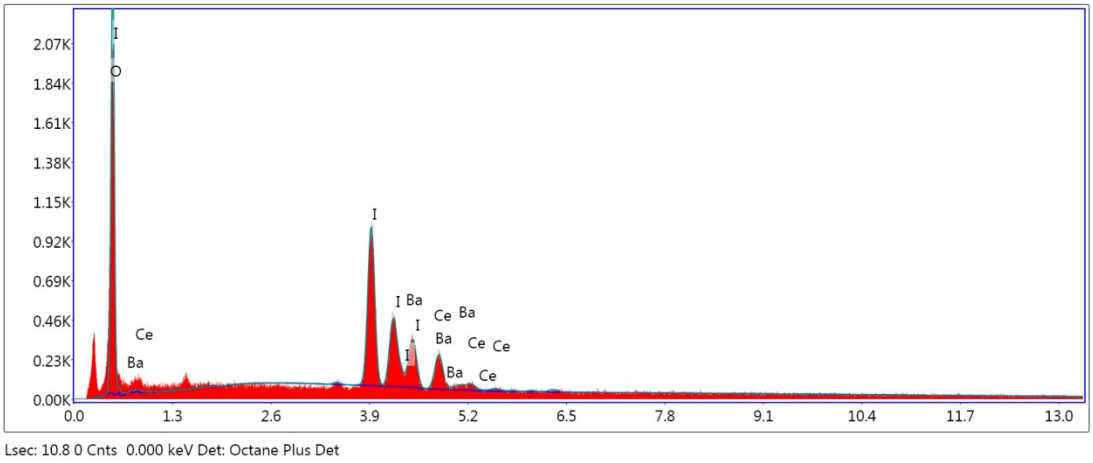

Figure S2. Energy dispersive spectroscopy analyses for $Ba_2Ce(IO_3)_8(H_2O)$.

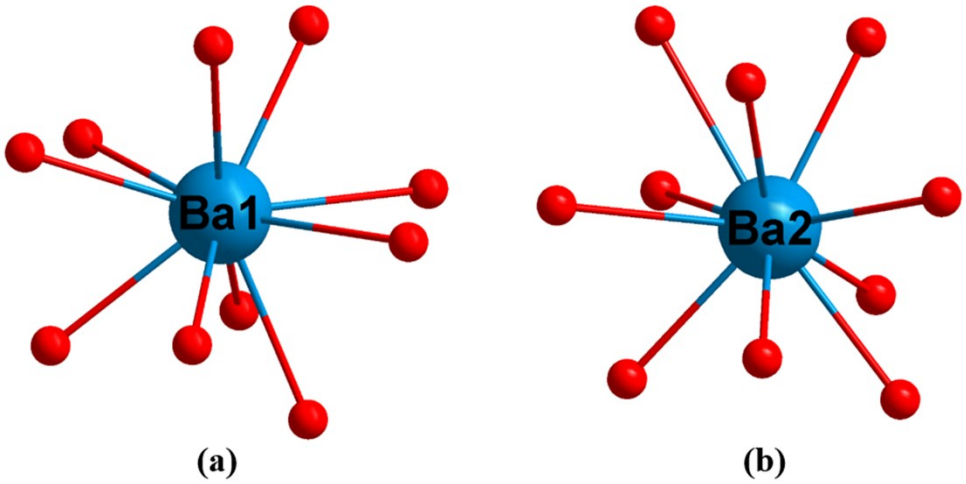

Figure S3. Coordination environment of $Ba(1)^{2+}$ (a) and $Ba(2)^{2+}$ (b).

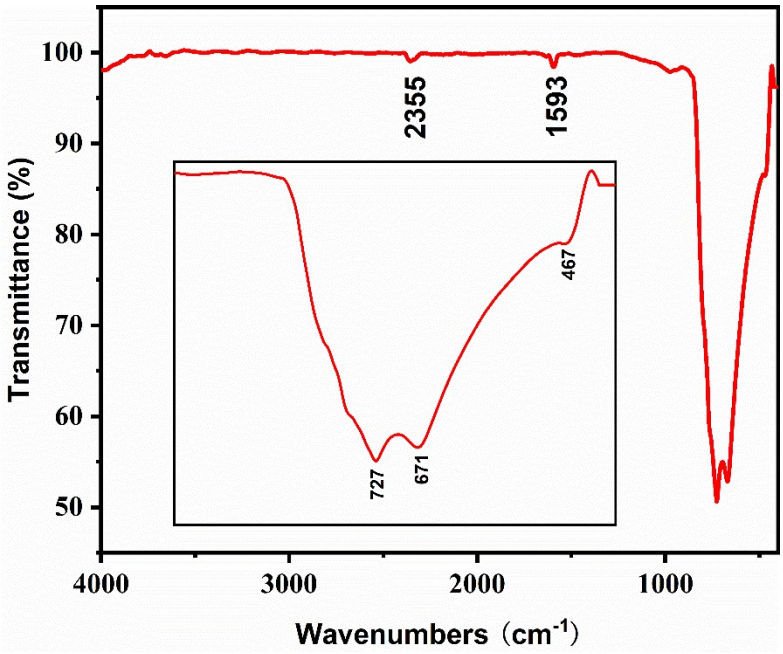

Figure S4. Infrared spectrum of $Ba_2Ce(IO_3)_8(H_2O)$.

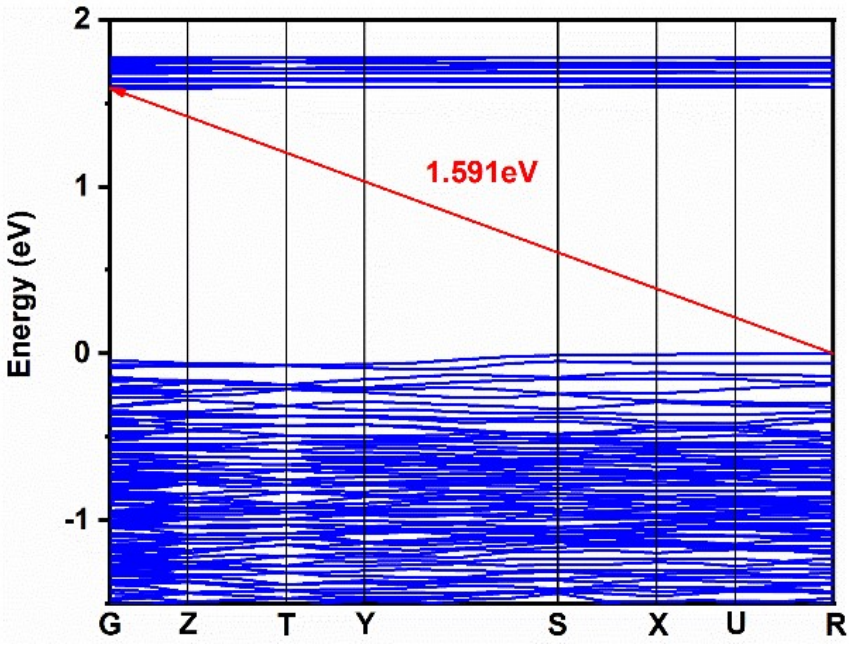

Figure S5. Calculated band structures of $Ba_2Ce(IO_3)_8(H_2O)$.

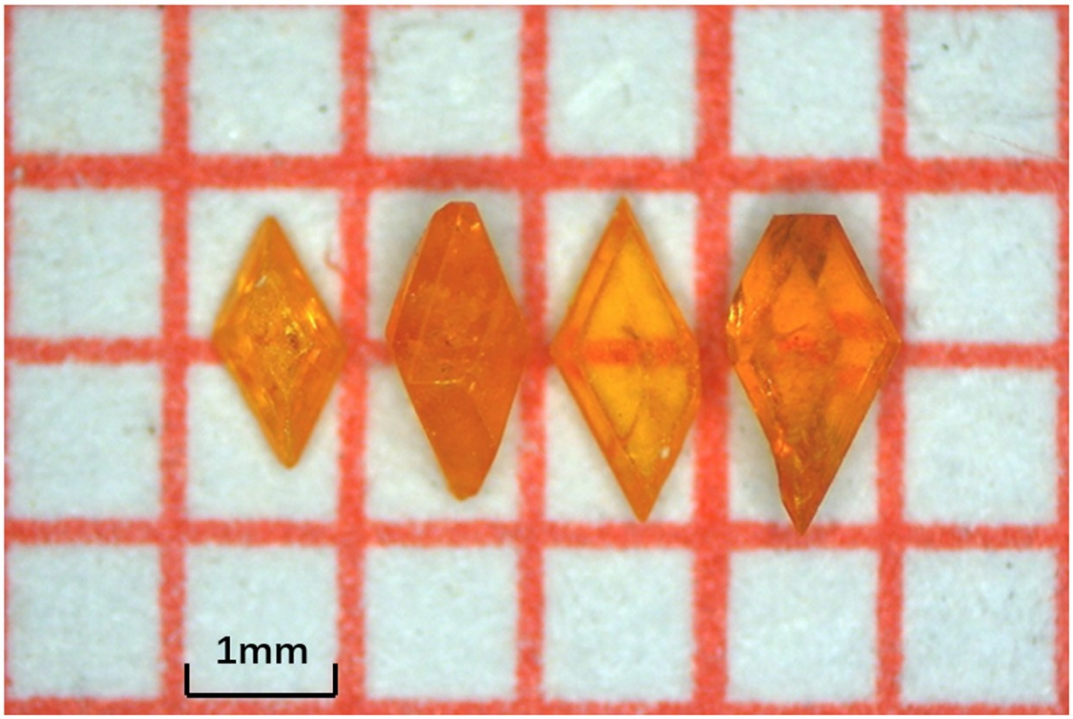

Figure S6. Photograph of $Ba_2Ce(IO_3)_8(H_2O)$ crystals.

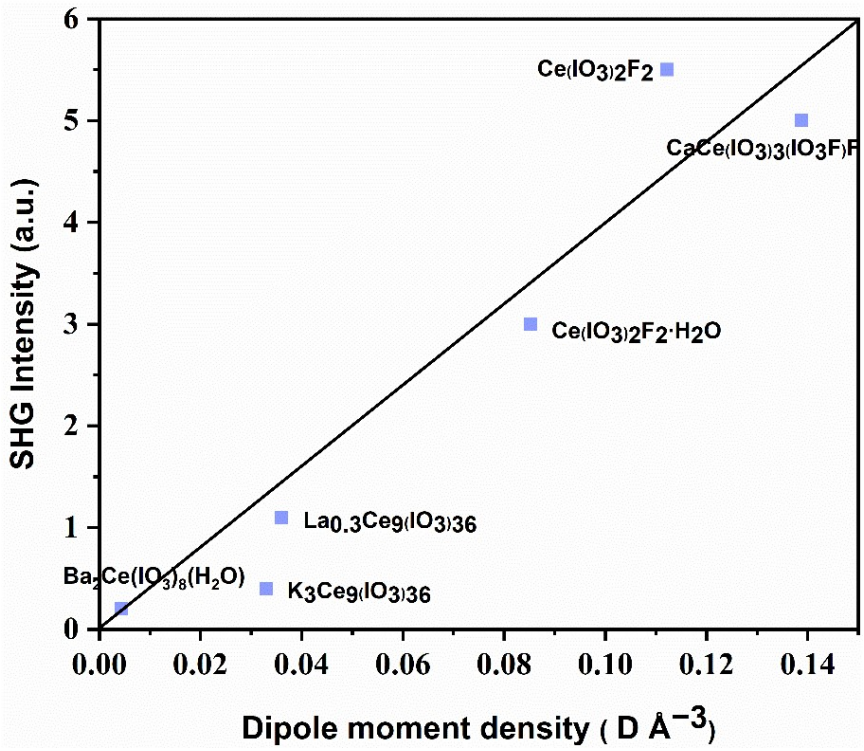

Figure S7. Comparison of the dipole moment density and the SHG effect of the reported cerium iodate NLO materials.

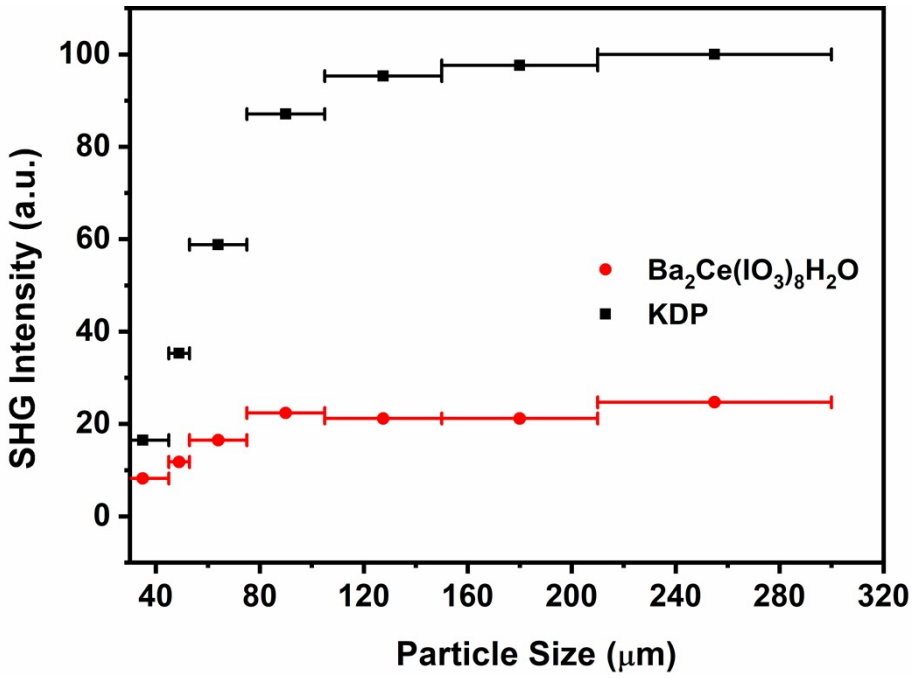

Figure S8. Plot of particle size versus SHG intensity of $Ba_2Ce(IO_3)_8(H_2O)$ under laser irradiation at λ = 1064 nm.

References

1. X. A. Chen, L. Zhang, X. A. Chang, H. G. Zang and W. Q. Xiao, *Acta Crystallogr., Sect. C: Cryst. Struct. Commun.*, 2005, **61**, I61-I62.
2. T. Eaton, J. Lin, J. N. Cross, J. T. Stritzinger and T. E. Albrecht-Schmitt, *Chem. Commun.* , 2014, **50**, 3668-3670.
3. S.-J. Oh, Hyung-Gu Kim, H. Jo, T. G. Lim, J. S. Yoo and K. M. Ok, *Inorg. Chem.*, 2017, **56**, 6973-6981.
4. J. Lin, Q. Liu, Z. Yue, K. Diefenbach, L. Cheng, Y. Lin and J. Q. Wang, *Dalton Trans*, 2019, **48**, 4823-4829.
5. T. Hu, L. Qin, F. Kong, Y. Zhou and J. G. Mao, *Inorg. Chem.*, 2009, **48**, 2193-2199.
6. L. Xiao, Z. B. Cao, J. Y. Yao, Z. S. Lin and Z. G. Hu, *J. Mater. Chem. C*, 2017, **5**, 2130-2134.
7. J. A. Ibers and D. T. Cromer, *Acta Crystallogr*, 1958, **11**, 794-798.
8. D. T. Cromer and A. C. Larson, *Acta Crystallogr*, 1956, **9**, 1015-1018.
9. Y. Wang, T. Duan, Z. Weng, J. Ling, X. Yin, L. Chen, D. Sheng, J. Diwu, Z. Chai, N. Liu and S. Wang, *Inorg. Chem.*, 2017, **56**, 13041-13050.
10. T. Abudouwufu, M. Zhang, S. C. Cheng, Z. H. Yang and S. L. Pan, *Chemistry*, 2019, **25**, 1221-1226.
11. R. E. Sykora, L. Deakin, A. Mar, S. Skanthakumar, L. Soderholm and T. E. Albrecht-Schmitt, *Chem. Mater.*, 2004, **16**, 1343-1349.
12. R. Wu, X. Jiang, M. Xia, L. Liu, X. Wang, Z. Lin and C. Chen, *Dalton Trans*, 2017, **46**, 4170-4173.
13. T. H. Wu, X. X. Jiang, Y. R. Zhang, Z. J. Wang, H. Y. Sha, C. Wu, Z. S. Lin, Z. P. Huang, X. F. Long, M. G. Humphrey and C. Zhang, *Chem. Mater.*, 2021, **33**, 9317-9325.
14. X. H. Zhang, B. P. Yang, C. L. Hu, J. Chen, Q. M. Huang and J. G. Mao, *Chem. Mater.*, 2021, **33**, 2894-2900.
15. N. Ma, C.-L. Hu, J Chen, Z Fang, Y. Huang, B.-X. Li and J.-G. Mao, *Inorg. Chem. Front.*, 2022, **9**, 5478-5485.
16. H. X. Tang, C. Zhuo, Y. X. Zhang, Q. R. Shui, R. B. Fu, Z. J. Ma and X. T. Wu, *Dalton Trans*, 2020, **49**, 3672-3675.